

Nuclear Trafficking of a Gadolinium Conjugate in Nude Mice Xenografted with Human LN-229 Glioma

Stefan Heckl and Ulrich Vogel

Department of Neuroradiology, University of Tübingen, Germany (S.H.),

Department of Pathology, University of Tübingen, Germany (U.V.)

Nuclear Trafficking of a Gadolinium Conjugate

corresponding author:

Stefan Heckl MD

Department of Neuroradiology, University of Tübingen, Medical School

Hoppe-Seyler-Str. 3, 72076 Tübingen

phone: 0049/07071/2986024

FAX: 0049/7071/689291

e-mail: stefan.heckl@med.uni-tuebingen.de

text pages: 25

tables: 1

figures: 3

supplemental figures: 1

references: 27

abstract: 119 words

introduction: 432 words

discussion: 627 words

Abbreviations: Gd, gadolinium; DTPA, diethylenetriamine pentaacetic acid ; SV, simian virus, Boc, t-butyloxy-carbonyl; OBut, t-butoxy; DMF, dimethylformamide; Mmt, 4-methoxytrityl, H&E, hematoxylin and eosin; TFA, trifluoroacetic acid

Non-standard abbreviations: FITC, fluorescein-isothiocyanate; diethylenetriamine pentaacetic acid; NLSs, nuclear localization sequences; ALL, acute lymphatic leukaemia; CLSM, confocal laser scanning microscopy; MRI, magnetic resonance imaging, DAB, 3,3'-diaminobenzidine tetrahydrochloride; Fmoc, 9-fluorenylmethoxycarbonyl-t-butyl; HBTU, 2-(1H-benzotriazole-1-yl)-1,1,3,3-tetramethyluronium hexafluorophosphate; ivDde, 4,4-dimethyl-2,6-dicyclohexyl-1-xylylidine-3-methylbutyl; Pbf, 2,2,4,6,7 pentamethyldihydro-benzofuran-5-sulfonyl; HPLC, high performance liquid chromatography

Abstract

We synthesized a novel fluorescein-isothiocyanate (FITC)-labeled gadolinium (Gd)-diethylenetriamine pentaacetic acid (DTPA) conjugate in which the commonly used gadolinium-DTPA complex is flanked by the nuclear localization sequences (NLSs) of the simian virus (SV)-40 T antigen and the acute lymphatic leukemia (ALL)-1 protein. The distribution of the conjugate after intraperitoneal or intravenous injection in nude mice bearing human LN-229 glioma xenografts was confirmed by magnetic resonance imaging (MRI), with an increase in signal intensity in all the organs and tumors except for healthy brain parenchyma with an intact blood-brain barrier. Nuclear uptake and efflux of the conjugate was demonstrated by confocal laser scanning microscopy (CLSM). Such gadolinium conjugates may therefore be of value in the development of novel diagnostic and therapeutic agents.

Introduction

The gadolinium (Gd)-diethylenetriamine pentaacetic acid (DTPA) complex, which is commonly used in routine clinical magnetic resonance imaging (MRI), is restricted to the extracellular space and cannot reach the cell nucleus. However, various potentially beneficial uses of the Gd-DTPA complex in the field of clinical diagnostics [e.g. the *in vivo* measurement of DNA repair enzyme activity in tumors prior to chemotherapy (Madhusudan and Middleton, 2005) and treatment (e.g. neutron capture therapy) (Martin et al., 1989; De Stasio et al., 2001)] would require the accumulation of a Gd-DTPA conjugate in the cell nucleus. It is therefore a matter of the utmost importance to develop small gadolinium conjugates that are able to cross the cell membrane without the need for large transmembrane transport peptides, and which can also enter the cell nucleus.

Nuclear localization sequences (NLSs) are short peptides that enable cytoplasmic proteins to enter the cell nucleus (Jans, 1995).

FITC-labeled NLSs can cross not only the nuclear membrane but also the cell membrane when added to the cell culture medium (Ragin et al., 2002).

We have developed a gadolinium conjugate composed of the gadolinium complex linked with two different NLSs (Table 1): the NLS of the simian virus (SV) 40 T antigen (Kalderon et al., 1984) and the NLS of the acute lymphatic leukemia (ALL)-1 protein (Yano et al., 1997), containing motifs of several other NLSs [e.g. Arginine-Lysine-Arginine of p21 (Rodriguez-Vilarrupla et al. 2002), Arginine-Lysine-Arginine-Lysine-Arginine of p45TC (Lorenzen et al., 1995) or Lysine-Arginine-Lysine-Arginine of PLAG1 (Braem et al., 2002)].

The NLS of the SV-40 T antigen was chosen because it is well known to mediate nuclear uptake of large cytoplasmic proteins. The second NLS, that of the ALL-1 protein, was linked to the Gd complex in order to mimic the positively charged residues (lysine, arginine) of the large transmembrane transport peptides like penetratin. It is postulated that these positively

charged residues, arranged along a β -sheet conformation, are predominantly responsible for the interaction of penetratin with the negatively charged phospholipids of the cell membrane, leading to cellular uptake (Binder and Lindblom, 2004; Christiaens et al., 2004).

Of course, an alternative would have been to use large polyarginine or polylysine chains, but such peptide sequences induce microvascular leakage of macromolecules in animals, polyarginine representing a surrogate for eosinophil basic proteins (Rosengren and Arfors, 1991; Minnicozzi et al., 1995).

We therefore chose to use a short peptide sequence consisting of alternating arginines and lysines.

Fluorescein isothiocyanate (FITC) was bound to the gadolinium conjugate to enable confirmation of nuclear localization by fluorescence microscopy. The conjugate was injected intraperitoneally and intravenously in nude mice bearing human LN-229 glioma xenografts.

Materials and Methods

Synthesis of the gadolinium conjugate

For the solid phase synthesis of the conjugate (Table 1) we employed the Fmoc (9-fluorenylmethoxycarbonyl-*t*-butyl) procedure (Merrifield, 1963; Carpino and Han, 1972) in a fully automated synthesizer (ABI 431) (Applied Biosystems, Weiterstadt, Germany) on 0.05 mmol Fmoc-Lys(Boc)-tritylchloride polystyrol (TCP) Resin (Trityl-Resin) (PepChem Tübingen, Germany) and on a 0.052 mmol Fmoc-Glu(OBut)-TCP Resin (Trityl-Resin). As coupling agent 2-(1H-Benzotriazole-1-yl)-1,1,3,3-tetramethyluronium hexafluorophosphate (HBTU) (Novabiochem, Bad Soden, Germany) was used. The side chains of trifunctional amino acids were protected as follows: Arg(Pbf), Lys(Boc), Lys(Mmt), Lys(ivDde), and Glu(OBut) [ivDde=4,4-dimethyl-2,6-dicyclohexyl-1-xylylidine-3-methylbutyl; Mmt=4-methoxytrityl; Pbf= 2,2,4,6,7 pentamethyldihydro-benzofuran-5-sulfonyl; Boc=*t*-butyloxy-carbonyl; OBut=*t*-butoxy] (Novabiochem, Bad Soden, Germany). We used Boc-Pro-OH (Novabiochem, Bad Soden, Germany) for coupling of the N-terminal amino acid.

The protected peptidyl resin was treated with 20% hexafluoroisopropanol (Merck, Darmstadt, Germany) in dicloromethane (SDS, Peypin, France) for 5-10 minutes and yielded a fully protected peptide.

The Mmt-protecting group was cleaved by treating it for 3 x 5 minutes in 1% trifluoroacetic acid (TFA) (Applied Biosystems, Weiterstadt, Germany) in dicloromethane and followed by coupling with 5(6)-carboxyfluorescein (FITC) (Novabiochem, Bad Soden, Germany). The ivDde-protecting group was cleaved with 4% hydrazine (Fluka, Buchs, Switzerland) in dimethylformamide (DMF) (SDS, Peypin, France). The DTPA was added as dianhydride (Merck, Darmstadt, Germany) and the coupling reaction lasted 6 hours.

The protection of the DTPA peptide was removed by treatment with 90% trifluoroacetic acid, 5% ethanedithiol (Fluka, Buchs, Switzerland), 2.5% thioanisol (Sigma-Aldrich, Taufkirchen,

Germany), and 2.5% phenol (Fisher Scientific, Schwerte, Germany) (v/v/v/v) for 2.5 h at room temperature. The products were precipitated in ether. The crude material was purified by preparatory high performance liquid chromatography (HPLC) (Shimadzu LC-8A, Japan) on an YMC-Pack ODS-AQ 120 Å, S-5µm reverse phase column (20 x 150 mm) using an eluent of 0.1% trifluoroacetic acid in water (A) and 60% acetonitrile (Fisher Scientific, Schwerte, Germany) in water (B). The peptide was eluted with a successive linear gradient of 25% B to 60% B in 40 min at a flow rate of 20 ml/min. The fractions corresponding to the purified protein were lyophilized.

The peptide was dissolved in a small amount of distilled water and added dropwise under stirring to a gadolinium solution [Gadolinium (III) chloride hexahydrate (Sigma Aldrich, Taufkirchen, Germany)] for a period of 1h. The pH was maintained at 5.8 by adding 0.1M NaOH. The solution was dialyzed until no free gadolinium was detected, using Xylenol-Orange (Fluka, Buchs, Switzerland) as indicator. The purified material was characterized by using analytical HPLC and laser desorption mass spectrometry, Vision 2000 (Finnigan MAT). Substance purity was 99%.

Tumor implantation

The animal experiments were approved by the Committee for Animal Experiments of the Regional Council (Regierungspräsidium), Tübingen and have been carried out in accordance with the Declaration of Helsinki and with the Guide for the Care and Use of Laboratory Animals as adopted and promulgated by the U.S. National Institutes of Health.

Athymic female nude mice (CD1 Nu/Nu) (weight: 25 g; age: 7 weeks) were purchased from Charles River (Sulzfeld, Germany). Human LN-229 glioma cells were maintained and implanted intracerebrally as described elsewhere (Friese et al., 2003). Investigations with the gadolinium conjugate were performed 4 weeks after tumor implantation.

Influx studies

The mice were subjected to intraperitoneal injection of 0.5 ml isotonic saline (2 animals), 0.5 mg FITC in 0.5 ml isotonic saline (2 animals), or 4 mg conjugate in 0.5 ml isotonic saline (4 animals) and killed after 60 minutes. The organs and brain tumors were excised and processed, as described below.

Efflux studies

To determine whether the conjugate also passes out of the cell nucleus, it was injected intraperitoneally into 6 animals, which were killed after 40 minutes (2 animals), 2.5 hours (2 animals), or 3 days (2 animals). The animals were not anesthetized at the time of injection or during the period of observation so that their behavior could be evaluated.

MRI measurements

The animals were sedated by intraperitoneal injection of ketamine (100 mg/kg) plus xylazine (10 mg/kg). They subsequently received an injection of 4 mg conjugate in 0.5 ml isotonic saline (intraperitoneal administration; 3 animals) or 3 mg conjugate in 0.25 ml isotonic saline (slow intravenous administration via the tail vein; 3 animals). MRI was then performed using a clinical 3 Tesla Siemens whole body MRI (Magnetom TRIO, Siemens; Erlangen, Germany) with the mice in prone position in a standard circular polarized wrist coil.

The imaging protocol for native and post-contrast scans consisted of:

3D turbo spin echo sequence: slice thickness 0.3125 mm, field of view read 63 mm, field of view phase 100.0%, base resolution 256, phase resolution 100%, slice resolution 100%, voxel size 0.2x0.2x0.3 mm, slab group 1, slabs 1, slices per slab 16, TR 300 ms, TE 15 ms, flip angle 70, distance factor 50, scan time 12:02 min.

T1 weighted transverse images: slice thickness 2mm, field of view read 31 mm, field of view phase 82.3 %, voxel size 0.2x0.2x2 mm, TR 600 ms, TE 18 ms, flip angle 180, number of slices 12, distance factor 0, scan time 11:35 min.

30 minutes after intravenous injection and 1 hour after intraperitoneal injection the animals were killed and the organs and brain tumors were excised and processed, as described below. MRI and CLSM scans of the tumors and organs were also obtained 30 minutes after intravenous injection of 0.25 ml isotonic saline alone (2 animals) and 1 hour after intraperitoneal injection of 0.5 ml isotonic saline alone (2 animals). These control animals were subsequently killed and the organs excised.

Techniques to evaluate nuclear uptake

In vivo fluorescence microscopy

Before injection of the conjugate (n=3) and isotonic saline alone (n=1), respectively, the skin of the nude mice was examined for green fluorescence using a fluorescence microscope (Axioskop, Carl Zeiss, Jena, Germany) with appropriate filters and beam splitters and an illuminator (N HBO103; Carl Zeiss, Jena, Germany). Pictures were taken with a 3-CCD color video camera (MC3254P, Sony, Japan) and the Axiovision software (Carl Zeiss, Jena, Germany). This examination was repeated 45 minutes after the injection in order to demonstrate peritoneal uptake and subsequent systemic distribution of the conjugate. The peritoneal cavity was then opened and the mesentery examined for nuclear fluorescence using the fluorescence microscope.

Touch prints

The organs were sliced immediately after excision for the preparation of touch print specimens, which were air-dried and examined with the fluorescence microscope.

Fresh frozen sections

Organ specimens were also snap-frozen in Tissue Tek OCT in liquid nitrogen. Frozen sections (4 μm) were prepared and evaluated using the fluorescence microscope and a confocal laser scanning microscope (LSM 410, Axiovert 135 M, Carl Zeiss, Jena, Germany). Cell nuclei were counterstained with TO-PRO-3 iodide (Molecular Probes, Eugene, OR, USA). For the fluorescence excitation of FITC and TO-PRO we used the 488 and the 633 nm line, respectively, of an argon ion and helium-neon laser, respectively, and appropriate beam splitters and barrier filters. Superimposed images of FITC- and TO-PRO-stained samples were created by overlaying coincident views. Hematoxylin and eosin (H&E) stained sections of these specimens were also prepared.

Semithin sections

Organ specimens were also fixed in paraformaldehyde, dehydrated in ethanol with progressive lowering of the temperature, embedded in Lowicryl K4M (Polysciences, Eppelheim, Germany) and UV-polymerized at -30°C according to the manufacturer's instructions. Semithin sections (about 0.4 μm) were examined with the fluorescence microscope.

Electron microscopy

Specimens were freeze-substituted at -30°C and then embedded in Lowicryl K4M (Polysciences, Eppelheim, Germany).

Immunoelectronmicroscopy was performed using a peroxidase-coupled primary anti-FITC antibody (Boehringer, Mannheim, Germany). The bound antibody was visualized with DAB (3,3'-diaminobenzidine tetrahydrochloride) (Roche, Mannheim, Germany).

Additionally, immunoelectronmicroscopy was performed using an 18-nm gold-labeled anti-FITC antibody (Dianova, Hamburg, Germany). Specimens were analyzed and documented using an EM 10A electron microscope (Zeiss, Oberkochen, Germany).

Results

Prior to administering the gadolinium conjugate, we excluded significant green autofluorescence of the skin (Fig. 1a) and mesentery (Fig. 1b) of the experimental animals by fluorescence microscopy after intraperitoneal injection of 0.5 ml of isotonic saline solution. Significant green autofluorescence of cell nuclei in the organs (lung, heart, liver, spleen, intestinal tract, skin, smooth and striated muscle, peritoneum, brain) and xenografted gliomas was also excluded by fluorescence microscopy and confocal laser scanning microscopy (CLSM) of fresh frozen specimens (Figs. 1c and 3c), touch prints and semithin sections (Fig. 1e) respectively. The intraperitoneal administration of FITC alone (0.5 mg FITC dissolved in 0.5 ml isotonic saline) also produced no increase in fluorescence of the cell nuclei (organs excised 1 hour after injection; Fig. 1c). However, after injection of the FITC-labeled gadolinium conjugate, strong green fluorescence of the skin was detected (Fig. 1a). Intravital fluorescence microscopy revealed strong green nuclear staining in the cells of the mesentery (Fig. 1b). Nuclear staining could also be demonstrated in the organs listed above and in the glioma cells by fluorescence microscopy and CLSM in touch prints, fresh frozen specimens and semithin sections (Fig. 1, c-e; Fig. 3, b and c). Thus, the same results were obtained by various different techniques.

We were also able to confirm nuclear efflux, in addition to influx.

Fig. 2 illustrates the strong fluorescence seen in renal cell nuclei 40 minutes after intraperitoneal injection of the conjugate in non-anesthetized nude mice. By 2.5 hours and 3 days after injection, only weak fluorescence was found in the cell nuclei (Fig. 2). The clinical and histological findings in the mice that had received the conjugate remained normal, indicating that it had had no toxic effect during the period of observation.

The conjugate was also detectable by electron microscopy and MRI after intraperitoneal and intravenous injection [increase in magnetic resonance signal intensity in the brain tumors and all the organs except for healthy brain parenchyma with an intact blood-brain barrier (Fig.3a and supplemental Fig.1)] and was rapidly excreted via the bile and urine.

Discussion

Various reports concerning cellular and nuclear uptake of Gd complexes have been published. At high concentrations (up to 25 mg/ml) and after long incubation times (up to 120 hours) the commercially available Gd-DTPA complex was found to be taken up into the cytoplasm and finally the nuclei of human glioma cells in vitro (De Stasio et al., 2001). However, it would not be possible to apply these concentrations and incubation times in vivo, so that this method does not seem to be a practicable possibility.

Gadolinium-tetraazacyclododecanetetraacetic acid (Gd-DOTA) complexes conjugated with HIV-1 Tat-derived membrane translocation peptides have been shown to be taken up by the nuclei of mammalian cells (Bhorade et al., 2000; Prantner et al., 2003).

However, the HIV-1 Tat protein induces apoptosis of hippocampal neurons in rats by a mechanism involving caspase activation (Kruman et al., 1998). Mice that had been given HIV-1 Tat Gd-DOTA conjugates intraperitoneally died 90 minutes later (Prantner et al., 2003).

In vitro nuclear uptake of the Gd-DTPA complex has also been accomplished by coupling to the SV-40T antigen NLS via a non-cleavable spacer. The NLS was, in turn, cleavably linked to penetratin via a cleavable disulfide bond. However, it was found that the conjugate cannot leave the cell nucleus (Heckl et al., 2002). Motexafin gadolinium (MGd), a synthetically expanded porphyrin containing Gd, was found to be taken up by at least 90% of glioblastoma cell nuclei after a long incubation time of 72 hours (de Stasio et al., 2006). However, only 15% of murine EMT 6 mammary sarcoma cell nuclei were stained after incubation for 45 hours and no nuclear uptake of MGd was achieved in murine Rif-1 fibrosarcoma cells (Woodburn, 2001).

We report findings concerning the nuclear influx and efflux of a novel gadolinium conjugate in a nude mouse model. The conjugate, produced by the binding of two NLSs to the gadolinium complex, could be transported not only across the nuclear membrane -as

expected- but also across the cell membrane. Interestingly, large transmembrane transport units like penetratin (Heckl et al., 2002) could be omitted, resulting in a comparatively small conjugate with a proportionally low peptide content for each gadolinium complex, which is the most important constituent of the conjugate, producing as it does the signal on MRI and representing the target for possible neutron capture therapy. It is unclear whether our conjugate of 3 kDa was taken up by the nucleus via an active transport mechanism (e.g. importin alpha or beta) or passive diffusion. It is thought that small molecules (<10 kDa) can pass freely through the nuclear pores (Wei et al., 2003). However, a gadolinium conjugate of comparable size (gadolinium complex bound to 16 arginine, about 3 kDa) (Allen and Meade, 2003) was found to remain in the cytoplasm and could not enter the nucleus.

To exclude the possibility of fixation-based artefactual relocation of the gadolinium conjugate to the cell nucleus, as demonstrated for small peptides (Richard et al., 2003), we used various different techniques that avoid the need for fixation: *in vivo* fluorescence microscopy, and methods employing touch prints and fresh frozen sections. These techniques produced the same results as investigations performed on semithin sections of fixed tissue.

The gadolinium conjugate described in this study enters a range of different cell types nonspecifically. However, to be of use in tumor therapy, targeting of specific cells by the conjugate would be desirable. It may be possible, for example, to construct gadolinium conjugates that are taken up by cell nuclei only in the presence of certain extracellular enzymes (e.g. matrix metalloproteinase-2) expressed predominantly by tumors, so that tumor-directed therapy can be achieved (Jiang et al., 2004).

In addition, studies need to be performed to evaluate whether similar results could be achieved with smaller Gd conjugates containing only one NLS.

References

Allen MJ and Meade TJ (2003) Synthesis and visualization of a membrane-permeable MRI contrast agent. *J Biol Inorg Chem* **8**: 746-750.

Bhorade R, Weissleder R, Nakakoshi T, Moore A, and Tung C-H (2000) Macrocyclic Chelators with Paramagnetic Cations Are Internalized into Mammalian Cells via a HIV-Tat Derived Membrane Translocation Peptide. *Bioconjug Chem* **11**: 301–305.

Binder H and Lindblom G (2004) A Molecular View on the Interaction of the Trojan Peptide Penetratin with the Polar Interface of Lipid Bilayers. *Biophys J* **87**: 332–343.

Braem CV, Kas K, Meyen E, Debiec-Rychter M, Van De Ven WJ and Voz ML (2002) Identification of a karyopherin alpha 2 recognition site in PLAG1, which functions as a nuclear localization signal. *J Biol Chem* **277**: 19673-19678.

Carpino LA and Han GY (1972) The 9-fluorenylmethoxycarbonyl amino-protecting group. *J Org Chem* **37**: 3404–3409.

Christiaens B, Grooten J, Reusens M, Joliot A, Goethals M, Vandekerckhove J, Prochiantz A, Rosseneu M. (2004) Membrane interaction and cellular internalization of penetratin peptides. *European Journal of Biochemistry* **271**: 1187-1197.

De Stasio G, Casalbore P, Pallini R, Gilbert B, Sanita F, Ciotti MT, Rosi G, Festinesi A, Larocca LM, Rinelli A, Perret D, Mogk DW, Perfetti P, Mehta MP and Mercanti D (2001)

Gadolinium in human glioblastoma cells for gadolinium neutron capture therapy. *Cancer Res* **61**: 4272-4277.

De Stasio G, Rajesh D, Ford J M., Daniels M J, Erhardt R J, Frazer BH, Tyliczszak T, Gilles MK, Conhaim RL, Howard S P, Fowler J F, Estève F and Mehta M P (2006) Motexafin-Gadolinium Taken Up *In vitro* by at Least 90% of Glioblastoma Cell Nuclei. *Clin Cancer Res* **12**: 206-213.

Friese MA, Platten M, Lutz SZ, Naumann U, Aulwurm S, Bischof F, Buhring HJ, Dichgans J, Rammensee HG, Steinle A and Weller M. (2003) MICA/NKG2D-mediated immunogene therapy of experimental gliomas. *Cancer Res* **63**: 8996-9006.

Heckl S, Debus J, Jenne J, Pipkorn R, Waldeck W, Spring H, Rastert R, von der Lieth, CW and Braun K (2002) CNN-Gd(3+) enables cell nucleus molecular imaging of prostate cancer cells: the last 600 nm. *Cancer Res* **62**: 7018-7024.

Jans DA (1995) The regulation of protein transport to the nucleus by phosphorylation. *Biochem J* **311**: 705-716.

Jiang T, Olson ES, Nguyen QT, Roy M, Jennings PA and Tsien RY (2004) Tumor imaging by means of proteolytic activation of cell-penetrating peptides. *Proc Natl Acad Sci U S A* **101**: 17867-17872.

Kalderon D, Roberts BL, Richardson WD and Smith AE (1984) A short amino acid sequence able to specify nuclear location. *Cell* **39**: 499-509.

Kruman II, Nath A and Mattson MP (1998) HIV-1 Protein Tat Induces Apoptosis of Hippocampal Neurons by a Mechanism Involving Caspase Activation, Calcium Overload, and Oxidative Stress. *Experimental Neurology* **154**: 276-288.

Lorenzen JA, Dadabay CY and Fischer EH (1995) COOH-terminal sequence motifs target the T cell protein tyrosine phosphatase to the ER and nucleus. *J Cell Biol* **131**: 631-643.

Madhusudan S and Middleton MR (2005) The emerging role of DNA repair proteins as predictive, prognostic and therapeutic targets in cancer. *Cancer Treat Rev* **31**: 603-617.

Martin RF, D' Cunha, G., Pardee M and Allen BJ (1989) Induction of DNA double-strand breaks by ¹⁵⁷Gd neutron capture. *Pigment Cell Res* **2**: 330-332.

Merrifield RB (1963) Solid phase peptide synthesis. I. The synthesis of a tetrapeptide. *J Amer Chem Soc* **85**: 2149-2154.

Minnicozzi M, Ramírez MM., Egan RW, Gleich GJ, Kobayashi I, Kim D and Durán WN (1995) Polyarginine and eosinophil-derived major basic protein increase microvascular permeability independently of histamine or nitric oxide release. *Microvasc Res* **50**: 56-70.

Prantner AM, Sharma V and Piwnica-Worms D (2003) Synthesis and Characterization of a Gd-DOTA-D-Permeation Peptide for Magnetic Resonance Relaxation Enhancement of Intracellular Targets. *Mol Imaging* **2**:333-241.

Ragin AD, Morgan RA and Chmielewski J (2002) Cellular import mediated by nuclear localization signal Peptide sequences. *Chem Biol* **9**: 943-948.

Richard JP, Melikov K, Vives E, Ramos C, Verbeure B, Gait MJ, Chernomordik LV and Lebleu B (2003) Cell-penetrating peptides. A reevaluation of the mechanism of cellular uptake. *J Biol Chem* **278**: 585-590.

Rodriguez-Vilarrupla A, Diaz C, Canela N, Rahn HP, Bachs O and Agell N (2002) Identification of the nuclear localization signal of p21(cip1) and consequences of its mutation on cell proliferation. *FEBS Lett* **531**: 319-323.

Rosengren S and Arfors KE (1991) Polycations induce microvascular leakage of macromolecules in hamster cheek pouch. *Inflammation* **15**:159-172.

Wei X, Henke VG, Strübing C, Brown EB and Clapham DE (2003) Real-Time Imaging of Nuclear Permeation by EGFP in Single Intact Cells. *Biophysical Journal* **84**: 1317-1327.

Woodburn KW (2001) Intracellular Localization of the Radiation Enhancer Motexafin Gadolinium Using Interferometric Fourier Fluorescence Microscopy. *J Pharmacol Exp Ther* **297**: 888-894.

Yano T, Nakamura T, Blechman J, Sorio C, Dang CV, Geiger B and Canaani E (1997) Nuclear punctate distribution of ALL-1 is conferred by distinct elements at the N terminus of the protein. *Proc Natl Acad Sci U S A* **94**: 7286-7291.

Footnotes

This study is supported by the Hertie Foundation for Brain Research

Legends for Figures

Fig.1.

Peritoneal resorption and nuclear uptake of the gadolinium conjugate

a

In vivo fluorescence of the skin without (isotonic saline alone) (left) and after administration of the gadolinium conjugate dissolved in isotonic saline solution (right)

b

In vivo fluorescence of the mesentery without (isotonic saline alone) (left) and after administration of the gadolinium conjugate dissolved in isotonic saline solution (right)

c

Fresh frozen sections evaluated by confocal laser scanning microscopy (CLSM):

Kidney (three left-hand columns) and lung (three right-hand columns) of nude mice 1 hour after intraperitoneal administration of isotonic saline alone (row 1), isotonic saline plus FITC (row 2), and isotonic saline plus the conjugate (row 3).

Left-hand column for each organ and row:

Nuclei are demonstrated by TO-PRO-3 (specific staining of cell nuclei)

Right-hand column for each organ and row:

Localization of the FITC-labeled conjugate or FITC alone.

Specimens in row 1 and 2 were scanned with high sensitivity to show the low signal intensity within the cell nuclei compared to the cytoplasm.

Middle column for each organ and row:

Superimposed FITC and TO-PRO-3 images clearly demonstrate the nuclear localization of the conjugate

Note the nuclear areas without fluorescence in rows 1 and 2

d

Fluorescence microscopy of touch print specimens of spleen (row 1) kidney (row 2) and tumor (row 3) (left: FITC-channel; middle: fusion; right: transmission).

e

Fluorescence microscopy of Lowicryl-embedded semithin sections of the kidney without (left) and after (right) administration of the gadolinium conjugate

Fig.2.

Influx and efflux of the conjugate by the cell nuclei

CLSM of the kidneys of nude mice

40 minutes [(row 1, magnification x400), row 2 (magnification x1000)],

2.5 hours (row 3, magnification x1000), and

3 days (row 4, magnification x1000)

after intraperitoneal injection.

Left-hand column: TO-PRO-3 image

Right-hand column: Staining of the cell nuclei with FITC

Middle column: Superimposed TO-PRO-3 and FITC images

Specimens in rows 3 and 4 were scanned with high sensitivity to show the low signal intensity in the cell nucleus compared to the cytoplasm.

Fig.3.

LN-229 glioma, orthotopic xenograft

a

T1-weighted coronal MR images (3D turbo spin echo, TR 300 ms, TE 15 ms) of human LN-229 gliomas in nude mice before (left) and 30 minutes after (right) intravenous injection of isotonic saline plus the conjugate showing the tumor mass in the right olfactory bulb.

Healthy brain parenchyma does not take up the gadolinium conjugate and shows no increase in signal intensity. In the tumor region, however, the blood brain barrier is damaged and the conjugate can leave the capillaries and reach the tumor cells.

Anatomical structures:

- 1 Eyes
- 2 Olfactory bulbs
- 3 Interhemispheric cleft
- 4 Brain hemispheres
- 5 Brain stem
- 6 Tumor in the right olfactory bulb

b

CLSM image of the LN-229 tumor margin one hour after intraperitoneal administration of isotonic saline plus the conjugate (left, area with cell nuclei stained green). The cell nuclei in the brain parenchyma with an intact blood-brain barrier are not stained (right, dark area).

Histological structures:

- 1 Cell nucleus
- 2 Tumor margin
- 3 Healthy brain parenchyma
- 4 Ventricle

c

CLSM images of human LN-229 gliomas in nude mice before (first row) and 1 hour after intraperitoneal injection of isotonic saline plus the conjugate (second row)

First column: Staining of the cell nuclei with TO-PRO-3

Second column: Superimposed TO-PRO-3 and FITC images

Third column: Staining of the cell nuclei of an LN-229 glioma with FITC

Supplemental Fig.1.

Electron Microscopic Image of the cell nuclei (kidney) without (a) and with (b) peroxidase-coupled primary anti-FITC antibody after DAB staining.

PKKKRKVK(GdDTPA)RK(FITC)*RKKRK*

PKKKRKV : NLS of SV-40 T antigen

RKKRK : NLS of ALL-1 protein

TABLE 1

Formula of the conjugate

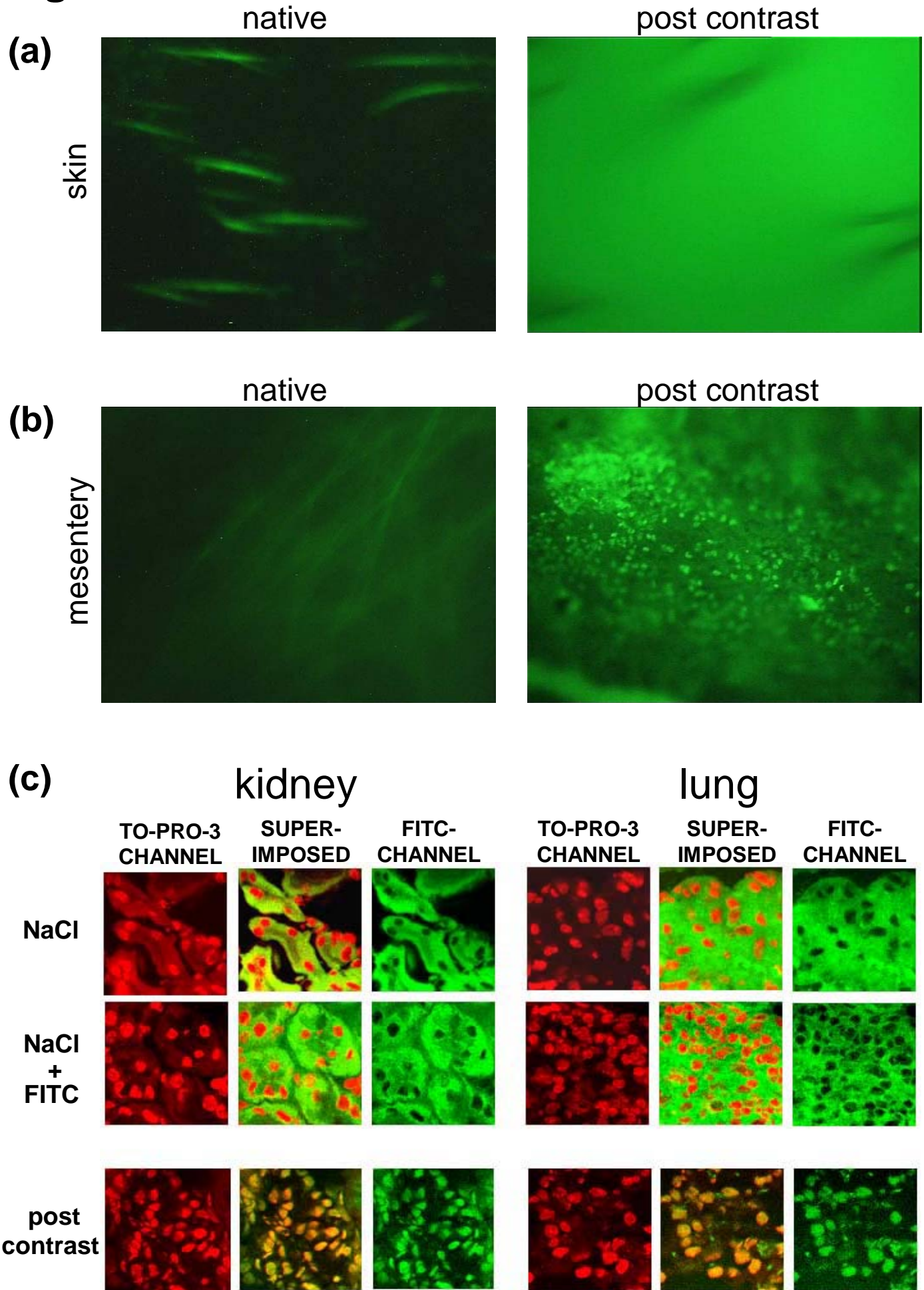
Single-letter amino acid code: K, lysine; R, arginine; P, proline; V, valine

Gd-DTPA, gadolinium-diethylenetriamine pentaacetic acid

FITC, fluorescein isothiocyanate

NLS, nuclear localization sequence

Fig.1.



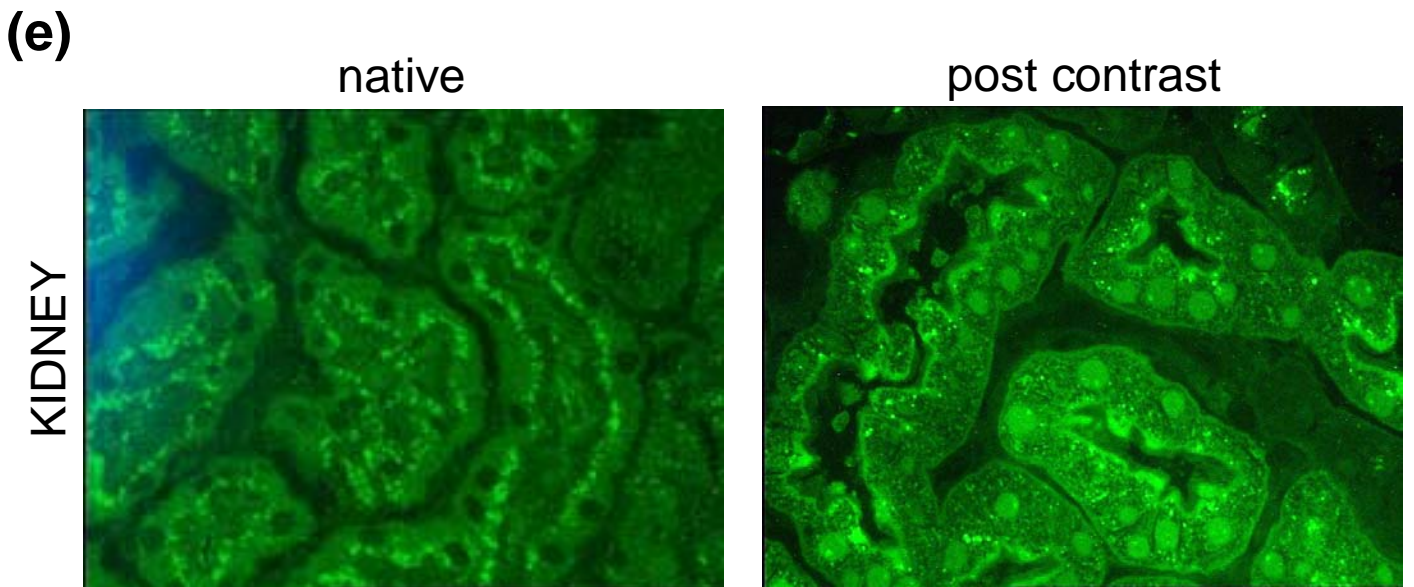
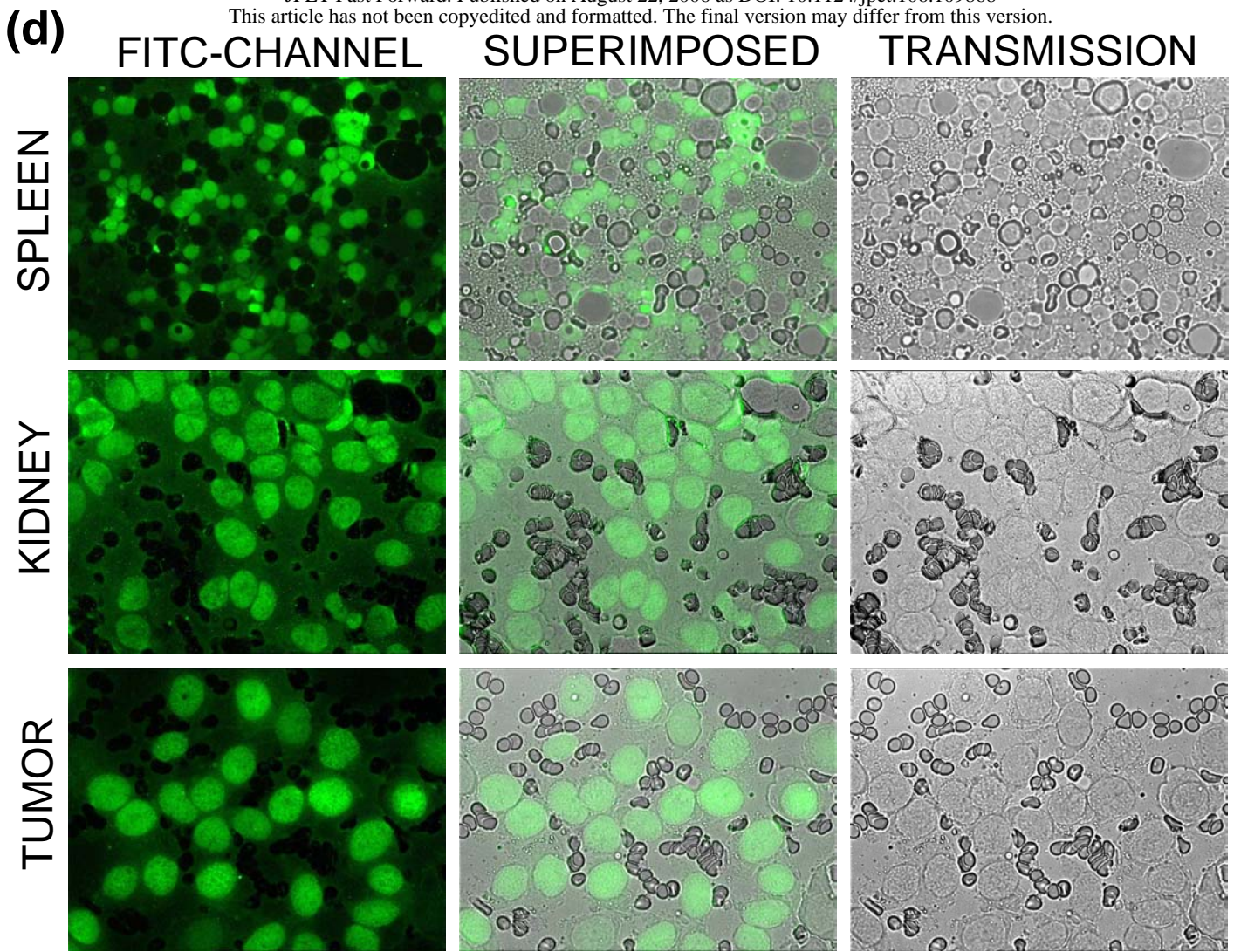


Fig.2.

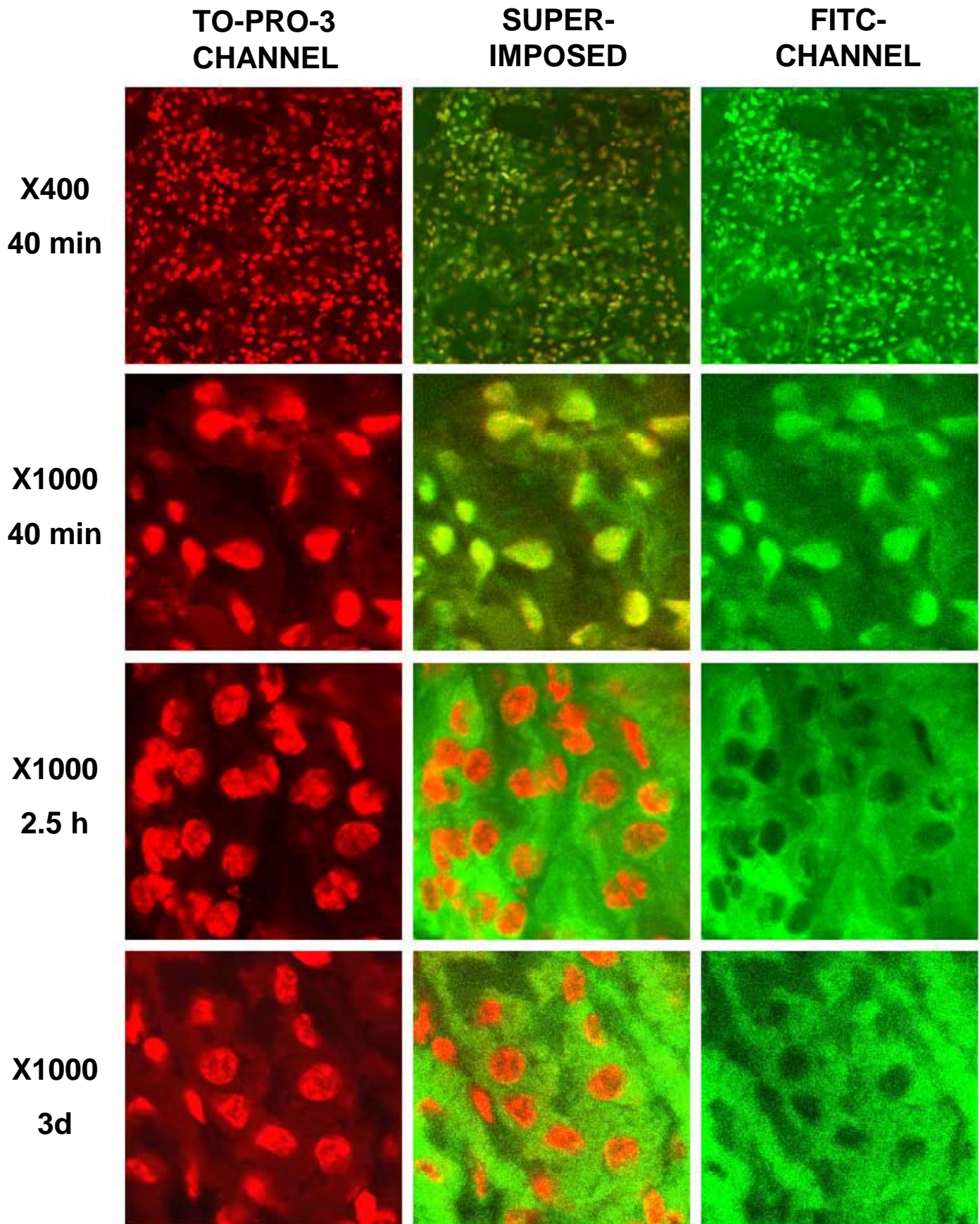
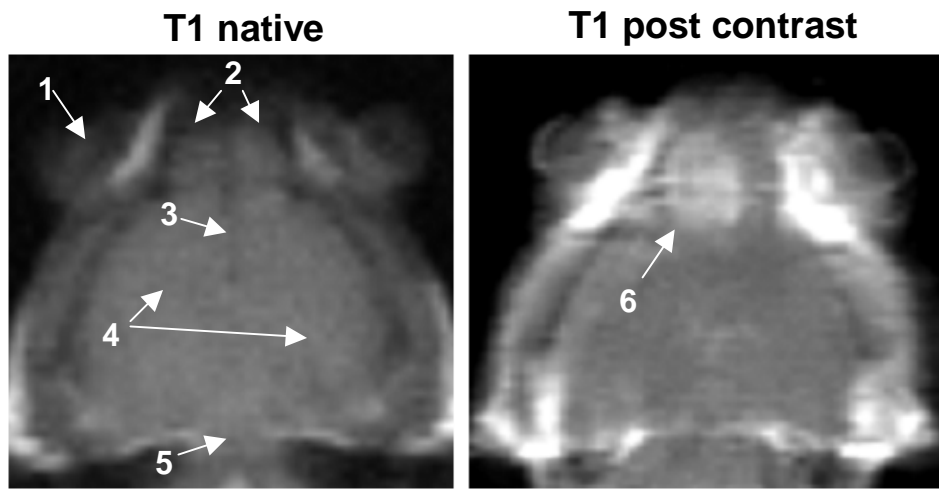
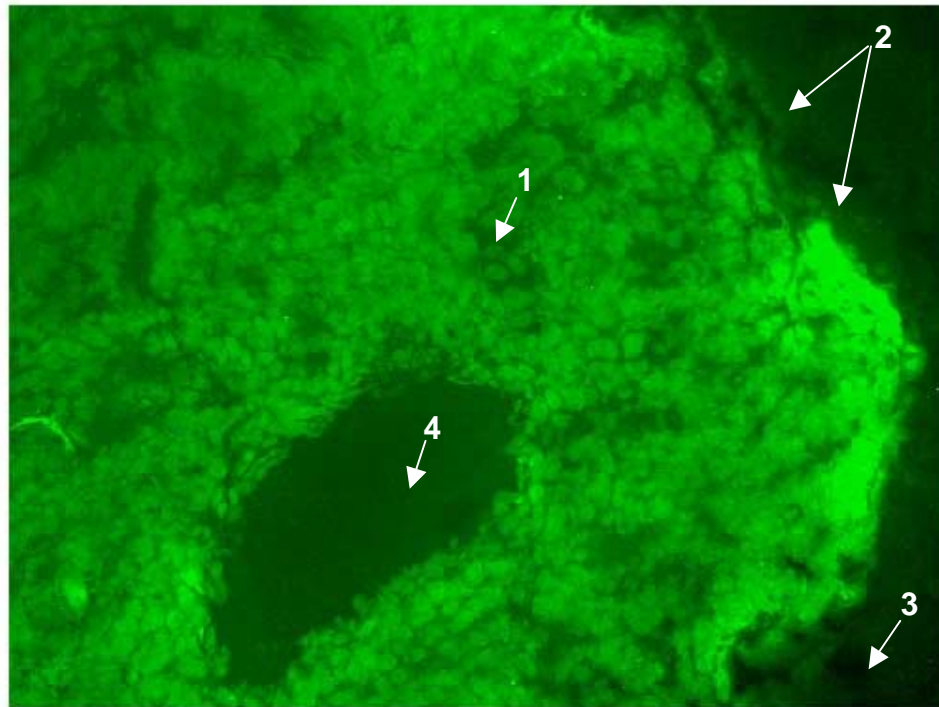


Fig.3.

(a)



(b)



(c)

